JOURNAL OF MATERIALS SCIENCE **37** (2002) 505–513

Relation between work of adhesion and work of fracture for simple interfaces

L. S. PENN*
Department of Chemical and Materials Engineering, University of Kentucky, Lexington, KY 40506-0046, USA
E-mail: penn@engr.uky.edu

E. DEFEX‡
Department of Chemical Engineering, Polytechnic University, Brooklyn, NY 11201, USA

A study was conducted of the relation between work of adhesion and work of fracture for adhesive-substrate systems exhibiting fracture at the interface. Materials and test conditions were selected to eliminate contributions from irreversible, energy-consuming processes in the bulk of the adhesive or substrate. Values for W_a were determined from contact angle measurements made at room temperature with the adhesive in the liquid state; values for $\boldsymbol{F}$ were determined from inverted blister tests conducted at temperatures low enough for the adhesive to be in the solid state. The independent variable, W_a, ranged from about 40 mJ/m^2 to 144 mJ/m^2. The dependent variable, $\boldsymbol{F}$, was found to range from 0.12 J/m^2 to 20 J/m^2, with most under 5 J/m^2. The excess of $\boldsymbol{F}$ over W_a was found to increase exponentially with W_a, and was proof of the occurrence of irreversible processes in specimens as they were loaded and fractured. The exponential behavior of ($\boldsymbol{F} - W_a$) with W_a suggested that the irreversible process was orientation hardening. The absence of detectable permanent deformation of any kind in the bulk substrates or at the fracture surfaces, plus the incapability of the adhesives to sustain significant irreversible processes, led to the conclusion that the orientation hardening must have taken place in the substrate, within a thin layer (and small volume) adjacent to the interfacial plane.

1. Introduction

In the field of adhesive-substrate interfaces and adhesive joints, there has been a longstanding interest in the relation between the thermodynamic work of adhesion, W_a, and total work of fracture, $\boldsymbol{F}$. Although the exact nature of the relation has not been elucidated, practical experience with adhesive bonding has shown that an increase in W_a usually leads to an increase in $\boldsymbol{F}$. A more thorough characterization of the relation between W_a and $\boldsymbol{F}$ could lead to better design of interfaces, and, as a result, tougher and more durable adhesive joints.

The present paper describes a study of the relation between W_a and $\boldsymbol{F}$ for adhesive-substrate systems exhibiting fracture at the interface. To keep the focus on processes at the interface, we took precautions to eliminate contributions to $\boldsymbol{F}$ from irreversible, energy-consuming processes arising from the bulk of either the adhesives or the substrates. To this end, low-molecular-weight compounds were used as adhesives. When in the solid state, these substances are brittle and elastic, and are incapable of exhibiting either viscoelastic yielding/plastic deformation, such as that found in glassy polymers, or mechanical hysteresis, such as that found in elastomers. In addition, extremely smooth-surfaced substrates were used. By precluding microscopic lock and key geometry, a smooth surface minimizes the true area of the interface, which, as a result, is more likely to fail before loads are reached that are high enough to initiate irreversible processes in the bulk.

The low-molecular-weight compounds selected as adhesives for this study had other advantages. Because of their diverse chemical structures, these compounds formed adhesive-substrate pairs that covered a wide range of W_a-values. Liquid at room temperature, the low-molecular-weight compounds could be subjected to contact angle measurements at ambient conditions for determination of W_a. Moreover, they could be solidified at low temperatures to form adhesive joints for experimental determination of $\boldsymbol{F}$. Finally, the low-molecular weight compounds used were relatively inert with respect to all the substrates, and could not form chemical bonds with, or diffuse into, the substrates. This eliminated irreversible interactions, such as interdiffusion and chemical reaction, from the interface, and limited the adhesion mechanism to intermolecular interactions, which are reversible.

*Author to whom all correspondence should be addressed.
‡*Present Address*: Pfizer Inc., Morris Plains, NJ, USA.

2. Theoretical background

The independent variable in this study was thermodynamic work of adhesion, W_a. Associated with joining (or separation) of two surfaces in a reversible process to form an interface, W_a is related to the surface free energies by the Dupre equation,

$$W_a = \gamma_s + \gamma_l - \gamma_{sl}, \tag{1}$$

where γ_s and γ_l are surface free energies of the solid and liquid separately, and γ_{sl} is the interfacial free energy. The contact angle, θ, made by a liquid on a clean, solid surface is related to the interfacial and surface free energies above by the Young equation,

$$\gamma_l \cos\theta = \gamma_s - \gamma_{sl}. \tag{2}$$

Equations 1 and 2 can be combined to form the very useful Young-Dupre equation,

$$W_a = \gamma_l (1 + \cos\theta). \tag{3}$$

Whenever both γ_l and θ can be measured experimentally, which could be done in our study, W_a can be computed from Equation 3 [1].

The dependent variable in this study was the work of fracture, $\boldsymbol{F}$. This quantity was determined from the inverted blister test, which is particularly suitable for use with brittle adhesives. In the inverted blister test, the substrate layer lies atop the adhesive [2–7], whereas in the traditional blister test, the adhesive layer lies atop the substrate [8–11]. The configuration of the inverted blister test is shown in Fig. 1, which also reveals that the substrate-adhesive bilayer is adhered to a massive base that is so thick, it has infinite stiffness. The base contains a central, cylindrical cavity that widens at the top to define a circular initial crack at the adhesive-substrate interface. The substrate sheet placed on top of, and made to adhere to, the adhesive layer closes the central cavity so that it can be pressurized with inert gas. Under pressurization, that portion of the substrate sheet (the nonadhered portion) directly over the central cavity is deflected upward. When a critical deflection is reached, the initial crack propagates at the adhesive-substrate interface.

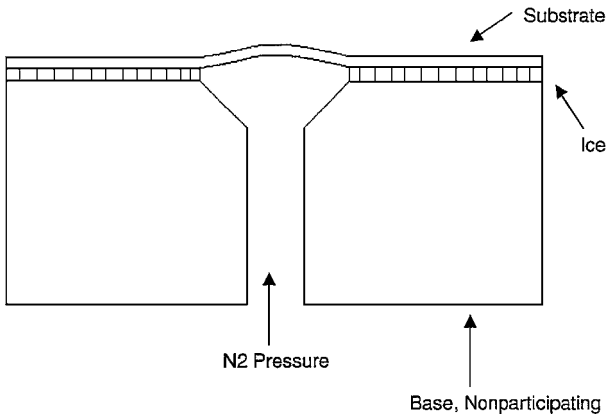

Figure 1 Schematic of inverted blister test. The substrate is on top, in the form of a sheet. The adhesive is the thin layer between the substrate and the massive base. The central hole in the base extends through the adhesive layer to meet the substrate. The initial crack in the adhesive-substrate interface is formed by the circular junction of adhesive layer and substrate. When the substrate is deflected upward by the pressure of inert gas, the initial crack propagates at the adhesive substrate interface.

The only part of the inverted blister test specimen that can store and then release energy is the substrate material that overlies the central hole and deflects upon pressurization. The base, because it is so stiff, stores negligible energy during the testing process. Thus, its properties can be ignored in the analysis of the test results. The adhesive layer, not only very thin, but also restrained between the massive base and overlying substrate sheet, cannot store any significant amount of energy during the testing process. Therefore, we can make the simplifying assumption that the mechanical properties of the adhesive can be ignored in the linear elastic analysis of the test. Andrews and Stevenson, in their analysis of the traditional blister test, treated the top layer as a clamped, circular plate that bends elastically with pressurization [11]. Then they assumed that strain energy in the top layer could be stored in two forms: near-field and far-field. Their analysis can be applied without change to the inverted blister test, in which the sheet of substrate is on top and the adhesive is underneath. The near-field strain energy due to local elastic deformation of the substrate near the crack tip is given by

$$U_n = \frac{4(1-\nu^2)}{3E} p^2 c^3, \tag{4}$$

where ν is the Poisson's ratio of the substrate, E is the Young's modulus of the substrate, p is the applied pressure, and c is the radius of the initial crack. The far-field strain energy comes from the upward deflection of the overlying sheet of substrate, and is given by

$$U_f = \frac{p^2\pi(1-\nu^2)}{32\,Eh^3}\left(c^6 + \frac{6h^2}{1-\nu}c^4\right), \tag{5}$$

where h is the thickness of the substrate and all other symbols are as in Equation 4.

The critical pressure, p_c, is the pressure at which the critical deflection of the circular plate is reached and the initial crack suddenly starts to propagate at the adhesive-substrate interface. The work of fracture, $\boldsymbol{F}$, can be computed by taking the derivative of the total stored energy of the system $(U_n + U_h)$ with respect to the interfacial area of fracture at constant pressure. The result is

$$\boldsymbol{F} = \frac{p_c^2 c(1-\nu^2)}{E}\left(\frac{3}{32}\left[\left(\frac{c}{h}\right)^3 + \left(\frac{c}{h}\right)\frac{4}{1-\nu}\right] + \frac{2}{\pi}\right). \tag{6}$$

Equation 6 can be rearranged to give

$$p_c = \sqrt{EF} \quad \sqrt{f(h/c)/c}, \tag{7}$$

where

$$f(h/c) = \frac{1}{1-\nu^2}\left(\frac{3}{32}\left[\left(\frac{c}{h}\right)^3 + \left(\frac{c}{h}\right)\frac{4}{1-\nu}\right] + \frac{2}{\pi}\right)^{-1}. \quad (8)$$

Equation 8 shows that different combinations of h and c can be used to provide a wide range of $f(h/c)$ over which linear elastic fracture mechanics can be applied. A plot of p_c versus $[f(h/c)/c)]^{1/2}$ is expected to give a straight line relation with a zero intercept and a slope equal to $(E\boldsymbol{F})^{1/2}$. The work of interfacial fracture, $\boldsymbol{F}$, can then be computed from the slope and the modulus, E, of the substrate. E must be determined separately. From Equation 7 it is clear that E, $\boldsymbol{F}$, and specimen geometry, $f(h/c)$, are separate influences on p_c, the quantity measured experimentally. It should be emphasized that $\boldsymbol{F}$ emerges in the analysis as a materials parameter, in the sense that it is independent of both E and specimen geometry.

3. Experimental

3.1. Materials

Low-molecular-weight organic liquids used as adhesives were obtained from Aldrich Co. (Minneapolis, MN) and were purified by column chromatography on powdered alumina (Fisher, Pittsburgh, PA) within an hour of use. Purified liquids were stored in a dessicator until ready for use. Water was triple-distilled in glass immediately before use. The surface tension of each liquid was measured with a platinum wire attached to a recording electronic microbalance [12]. The liquids, their surface tensions, and their melting points are listed in Table I.

Hexadecane, α-bromonaphthalene, and diiodomethane are hydrophobic substances, whereas water is hydrophilic. At the beginning of our study, attempts were made to include other hydrophilic liquids: formamide, ethylene glycol, and dimethyl acetamide. However, their propensity to absorb moisture from the air in the cold room lowered their freezing points so much that they could not freeze completely, even at -23°C. Therefore, these liquids were not studied further.

The solid plastics used as substrates were obtained in sheet form, with microscopically smooth surfaces, from Cadillac Plastic and Chemical Co. (New York, NY). The steel used as a substrate was obtained as shim stock in sheet form, with microscopically smooth surfaces, from Precision Co. (Downers Grove, IL). All substrates were washed with mild detergent, rinsed well, and dried before use. Thickness dimensions, tensile moduli at -20°C, and glass transition temperatures of the substrates are listed in Table II. The values shown for tensile moduli -20°C and at room temperature had been determined previously [6]. The values shown in Table II are low compared with literature values. This is because it was not possible to use strain gages or extensometers in the low-temperature measurements, and, as a consequence, the modulus values contain a contribution from compliance of the load train. However, the relative values and trends are reliable. In addition, the value measured at -20°C differed little from the value measured at room temperature for each substrate, so it was deemed unnecessary to measure modulus at every test temperature in between.

TABLE I Liquids and their surface tensions and melting points

Liquid	γ_L, mJ/m^2	m.p., °C
Water	72.8	0.0
Formamide	58.2	2.3
Diiodomethane	50.8	6.0
Ethylene glycol	48.2	−13
Bromonaphthalene	43.9	−1.0
Dimethyl acetamide	35.4	−20
Hexadecane	27.6	18

TABLE II Substrates and their thickness, moduli, and glass transition temperatures

Substrate	Thickness, mm	E at -20°C, GPa[a]	T_g, °C
Polytetrafluoroethylene	1.58, 3.15	1.32 ± 0.14	120
Polystyrene	1.53	1.30 ± 0.07	110
Polymethyl methacrylate	1.60	1.77 ± 0.12	100
Polycarbonate	1.70	1.43 ± 0.12	140
Steel	0.25, 0.30, 0.38, 0.64	33.4 ± 4.0	—

[a]Average ±1 std. deviation.

3.2. Work of adhesion

The sessile drop method was used for contact angle measurements of each liquid adhesive on each solid substrate. Advancing contact angles at room temperature were measured directly on the various substrates at room temperature by means of a custom-made contact angle goniometer. The value for work of adhesion of each adhesive-substrate pair was computed from Equation 1.

3.3. Work of interfacial fracture

Before presenting the procedures for preparation and testing of inverted blister specimens, we wish to emphasize that working at the extremely low temperatures used in this study was accompanied by several severe technical limitations. Standard electronic monitoring and data acquisition equipment could not be exposed to prolonged periods at low temperatures. Microscopes could not be used in the cold room, and liquids could not be used for pressurization because they either solidified or became too thick.

Twelve massive, cylindrical bases that could be reused as often as needed were machined from aluminum. A centrally located, cylindrical cavity was machined into each base (Fig. 1). All cavities had the same standard diameter at the bottom, but each tapered to a different diameter at the top. The diameter at the top defined the size of the initial, circular crack at the adhesive-substrate interface of the blister specimens made subsequently from each base. Thus, the twelve massive bases provided twelve initial crack radii, c, ranging

from 0.61 mm to 1.50 mm. Various combinations of c and h (substrate thickness in Table II) were used to achieve a wide range of values for the geometry function, $f(h/c)$.

An individual inverted blister specimen was prepared as follows. The top surface of the massive base (aluminum) was cleaned with mild detergent solution, rinsed, and wiped dry. The base was then placed for one hour in a variable-temperature cold room, the temperature of which was set at the freezing point of the liquid adhesive. All subsequent steps were conducted in the cold room. Five to six drops of the liquid adhesive were placed on top of the base with a pipette, and the substrate sheet was immediately placed on top of the drops and pushed down gently. Under this gentle pressure, the liquid drops coalesced into a continuous thin layer, no more than 0.20 mm thick. Any excess liquid that squeezed out during this process was trapped in the small, machined step at the top of the central cavity (Fig. 1). Liquid trapped in the step was carefully removed by suction through a tiny rubber tube inserted from below with the aid of a small mirror. This procedure ensured that the adhesive layer terminated precisely at the top of the central cavity, producing a circular initial crack with no irregularities at the adhesive-substrate interface. (An initial crack produced in this way would be more like a bimaterial corner than a sharp initial crack.) Once the substrate and adhesive were properly in place, the temperature of the cold room was lowered to the desired test temperature below the freezing point of the liquid and was held there for at least two hours before the specimen was tested.

Mechanical testing of the inverted blister specimens was conducted in the cold room at temperatures approximately 10° and 20°C below the freezing points of the low-molecular-weight compounds used as adhesives. A cylinder of compressed, inert gas was coupled by means of metal tubing and a threaded connector to the bottom of the central hole in the massive base. Pressurization of the central cavity was controlled manually with the aid of an operating valve and four pressure gauges, calibrated so their ranges overlapped. Our equipment permitted control of the pressurization rate but not the gas volume. The pressure was increased at rate of 18.6 kPa/sec until it reached a maximum, after which it dropped suddenly to zero. This maximum in pressure, designated p_c, marked the propagation of the initial crack and was reached within 2 to 15 seconds, the shorter times corresponding to larger initial cracks. Since crack growth was catastrophic, completely separating the overlying substrate layer from the adhesive layer, only one value of p_c could be obtained per specimen.

Immediately after the test, each specimen was examined (in the cold room) to determine the locus of failure. Interfacial failure was easy to distinguish from cohesive failure within the adhesive material because of the great difference in reflectivity of the surfaces of substrates with and without residual adhesive. In addition, the fracture surfaces were examined for evidence of any plastic deformation or viscoelastic yielding. This was done by checking the flatness of both adhesive and substrate with a delicate probe, and by remeasuring the thickness of the substrate.

Test results from specimens with different combinations of h and c were used to make a plot of p_c versus $[f(h/c)/c]^{1/2}$ for each adhesive-substrate system at each temperature. $\boldsymbol{F}$ was computed from the slope, $(E\boldsymbol{F})^{1/2}$, of each plot with knowledge of the modulus, E, of the substrate at low temperature (see Table II). Figs 2–4 show typical examples of the plots from which $\boldsymbol{F}$ was computed. Each point in the plots represents an individual inverted blister test. The correlation between the two variables, p_c and $[f(h/c)/c]^{1/2}$, was evaluated by a linear regression. The high correlation coefficient, R, shown in each figure indicates that use of an energy balance criterion based on linear elastic theory was appropriate. The low scatter around the regression line indicates that the reproducibility of the test was good, and that the value of $\boldsymbol{F}$ was not significantly influenced by initial crack size, c, or by substrate thickness, h. However, according to Equation 7, which has no second term, the regression line should go through zero, but it does not. The regression line intercepts the y-axis below zero, even when the experimental scatter in the data is considered. The most likely cause of this nonzero intercept is residual stress developed during the cooldown stage of specimen preparation. Residual stress between adhesive and substrate with different coefficients of thermal contraction is a well known phenomenon in adhesive joints, and has been discussed for specimens prepared at elevated temperatures and cooled to room temperature for testing [13]. The bond-weakening effect of thermal residual stress would cause a similar reduction in the

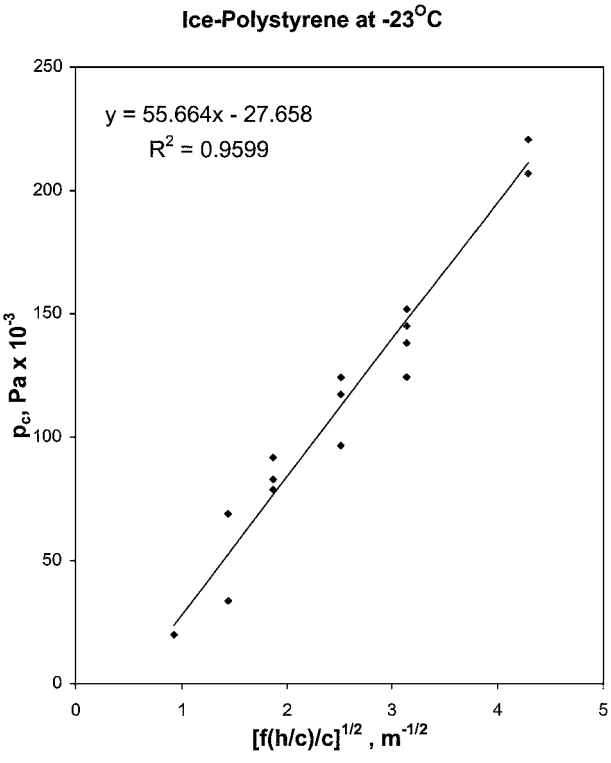

Figure 2 Plot of p_c versus $[f(h/c)/c]^{1/2}$ for inverted blister test on ice-polystyrene interface at −23°C. Each data point is from an individual test. Work of interfacial fracture, $\boldsymbol{F}$, was computed from the slope.

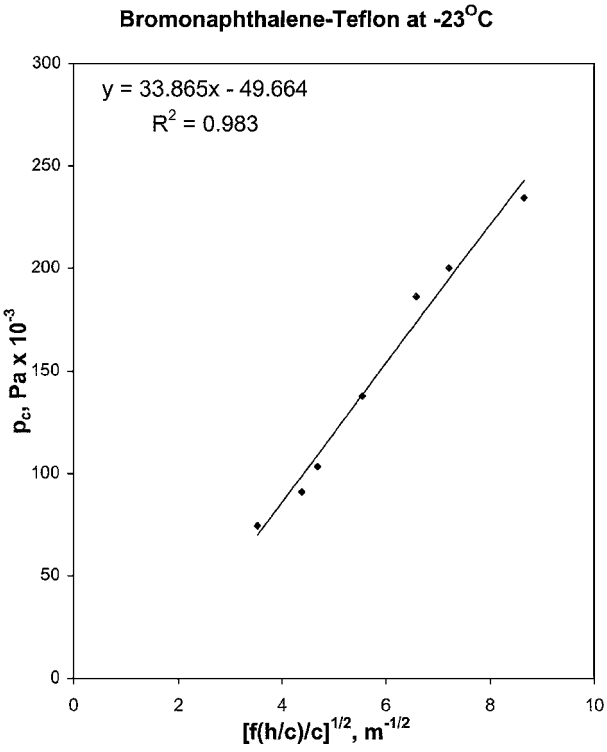

Figure 3 Plot of p_c versus $[f(h/c)/c]^{1/2}$ for inverted blister test on bromonaphthalene-Teflon (tetrafluoroethylene) interface at −23°C. Each data point is from an individual test. Work of interfacial fracture, $\boldsymbol{F}$, was computed from the slope.

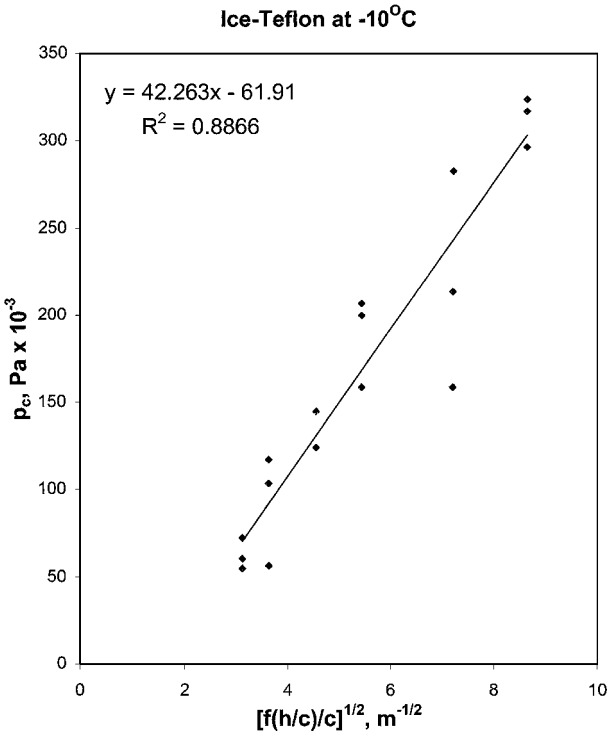

Figure 4 Plot of p_c versus $[f(h/c)/c]^{1/2}$ for inverted blister test on ice-Teflon (tetrafluoroethylene) interface. Each data point is from an individual test. Work of interfacial fracture, F, was computed from the slope.

p_c-values of all specimens of a given adhesive-substrate pair, shifting the regression line uniformly downward, but leaving the slope unchanged. Since the value of $\boldsymbol{F}$ for each adhesive-substrate pair is computed from the slope, residual stress would not affect the trends observed or the conclusions drawn in this study.

Another possible influence on p_c, opposite in direction from residual stress, was the lack of infinite sharpness in our initial cracks. This lack of sharpness in the initial cracks would be expected to elevate the measured values of p_c slightly, but it would do so consistently for all specimens, and therefore would not affect the trends observed or the conclusions drawn in this study. In the final analysis, however, the lack of sharpness of the initial cracks was inconsequential compared to the effect of residual stress, because the regression lines for all adhesive-substrate pairs were shifted downward rather than upward relative to the ideal case described by Equation 7, in which the line must be positioned to go through zero.

4. Results and discussion

The values obtained for work of adhesion, W_a, for all the adhesive-substrate systems used in this study are presented in Table III. These values range from about 40 mJ/m^2 to 144 mJ/m^2 and do not parallel the trend in surface tensions given in Table I. Such parallelism is not expected, because W_a is a function not only of γ_l but also of $\cos\theta$, the latter of which is determined by the detailed intermolecular interactions across the interface between the liquid and the solid it contacts. The numerical value of W_a for a given adhesive-substrate system depends on the exact magnitude of the various kinds of intermolecular interactions present at the interface. For more discussion of the influence of chemical structure on W_a, interested readers should consult texts on surface energetics [e.g., 14].

Table III also presents the values obtained for work of fracture, $\boldsymbol{F}$, for the various adhesive-substrate systems used in this study. The temperatures shown in the table are those at which inverted blister tests were conducted. As expected, neither viscoelastic yielding nor plastic deformation was found in the bulk. The debonded surfaces also appeared smooth and flat, and showed no evidence of plastic deformation or viscoelastic yielding. For most of the adhesive-substrate systems, the fracture path was completely interfacial, and the surfaces of the debonded substrates showed no traces whatsoever of residual adhesive. However, cohesive fracture within the adhesive occurred frequently for bromonaphthalene and hexadecane, and these cases are noted in Table III. Since our purpose was to study fracture at the interface, we do not list $\boldsymbol{F}$-values for the cases of cohesive fracture.

The values of $\boldsymbol{F}$ obtained in our study (Table III) ranged from 0.12 J/m^2 to 20 J/m^2, and most were below 5 J/m^2. Compared with values obtained for separation of typical polymer adhesives from metal substrates, which include energy dissipated by irreversible processes in the bulk, the values in Table III are very low. This can be attributed not only to the absence of irreversible processes such as viscoelastic yielding or plastic deformation in the bulk, but also to the absence of certain irreversible processes that are typically found localized at the interface, such as breaking of chemical bonds, polymer chain pull-out, or fracture of microscopic mechanical interlocks.

TABLE III Summary of work of adhesion, interfacial fracture energy, and test temperatures for all systems

Adhesive	Substrate	T, °C	W_a, mJ/m^2	$\boldsymbol{F}$, mJ/m^2
Water (ice)	Polytetrafluoroethylene	−23	44.8	564 ± 92
Water (ice)	Polystyrene	−23	70.1	1970 ± 210
Water (ice)	Polymethyl methaccrylate	−23	84.7	5820 ± 760
Water (ice)	Polycarbonate	−23	101.7	1910 ± 290
Water (ice)	Steel	−23	144.4	19300 ± 3300
Water (ice)	Polytetrafluorethylene	−10	44.8	120 ± 210
Water (ice)	Polystyrene	−10	70.1	730 ± 620
Water (ice)	Polymethyl methacrylate	−10	84.7	3310 ± 63
Water (ice)	Polycarbonate	−10	101.7	729 ± 170
Water (ice)	Steel	−10	144.4	16300 ± 3030
Diiodomethane	Polytetrafluoroethylene	−23	39.7	218 ± 59
Diiodomethane	Polystyrene	−23	86.5	—[a]
Diiodomethane	Polymethyl methacrylate	−23	89.1	1490 ± 678
Diiodomethane	Polycarbonate	−23	86.8	621 ± 134
Diiodomethane	Steel	−23	101.6	2490 ± 579
Diiodomethane	Polytetrafluoroethylene	−16	39.7	792 ± 140
Diiodomethane	Polystyrene	−16	86.5	—[a]
Diiodomethane	Polymethyl methacrylate	−16	89.1	1810 ± 51
Diiodomethane	Polycarbonate	−16	86.8	2246 ± 520
Diiodomethane	Steel	−16	101.6	4710 ± 1100
Diiodomethane	Polytetrafluoroethylene	−6	39.7	705 ± 110
Diiodomethane	Polystyrene	−6	86.5	—[b]
Diiodomethane	Polymethyl methacrylate	−6	89.1	1240 ± 190
Diiodomethane	Polycarbonate	−6	86.8	1540 ± 280
Diiodomethane	Steel	−6	101.6	—[a]
Bromonaphthalene	Polytetrafluoroethylene	−23	55.0	719 ± 85
Bromonaphthalene	Polystyrene	−23	79.9	—[a]
Bromonaphthalene	Polymethyl methacrylate	−23	88.4	655 ± 99
Bromonaphthalene	Polycarbonate	−23	87.3	—[a]
Bromonaphthalene	Steel	−23	89.2	1120 ± 102
Bromonaphthalene	Polytetrafluoroethylene	−10	55.0	—[a]
Bromonaphthalene	Polystyrene	−10	79.9	—[b]
Bromonaphthalene	Polymethyl methacrylate	−10	88.4	—[a]
Bromonaphthalene	Polycarbonate	−10	87.3	—[b]
Bromonaphthalene	Steel	−10	89.2	—[a]
Hexadecane	Polytetrafluoroethylene	−4	45.0	—[a]
Hexadecane	Polystyrene	−4	55.2	—[a]
Hexadecane	Polymethyl methacrylate	−4	—	—[a]
Hexadecane	Polycarbonate	−4	54.9	—[a]
Hexadecane	Steel	−4	55.4	—[a]
Hexadecane	Polytetrafluoroethylene	+5	45.0	287 ± 53
Hexadecane	Polystyrene	+5	55.2	—[a]
Hexadecane	Polymethyl methacrylate	+5	—	—[a]
Hexadecane	Polycarbonate	+5	54.9	—[a]
Hexadecane	Steel	+5	55.4	—[a]

[a]Adhesive did solidify but exhibited cohesive fracture, not interfacial fracture.
[b]Adhesive in the liquid state interacted with solid substrate.

Values reported recently by Liechti *et al*. for the separation of thin polymer films from aluminum substrates at room temperature in the traditional blister test configuration ranged from approximately 500 to 1000 J/m^2 [15–17]. When the contributions from global viscoelastic yielding in the specimens were deducted, the values ranged from 390 to 750 J/m^2. Even though these last values exclude contributions from irreversible processes in the bulk, they still significantly exceed the values obtained in our study. The reason for this is that the interfaces in the Liechti study were formed from a reactive adhesive (polyimide) and a geometrically complex metal oxide surface, whereas the interfaces in our study were simple and microscopically planar. It is almost certain that fracture of the interfaces prepared by Liechti *et al*. involved local irreversible processes such as breaking of chemical bonds and polymer chain pull-out from the oxide microstructure, whereas fracture along the interfaces in our study involved none of these.

Even though we were able to eliminate irreversible processes from the bulk and most of the irreversible processes from the interface, the $\boldsymbol{F}$-values obtained in our study still exceeded the W_a-values. This excess, expressed as $(\boldsymbol{F} - W_a)$, indicates that irreversible, energy-consuming processes of some kind were taking place in our specimens. Since these processes were obviously not occurring in the bulk, they must have been taking place *in the interfacial region*. We sought clues to the nature of the process responsible for the excess energy by focusing on the behavior of $\boldsymbol{F}$ as a function of W_a.

When $\boldsymbol{F}$ and W_a are plotted against each other, it is apparent that $\boldsymbol{F}$ is an increasing function of W_a. Fig. 5 shows $\boldsymbol{F}$ versus W_a for the hydrophobic adhesives,

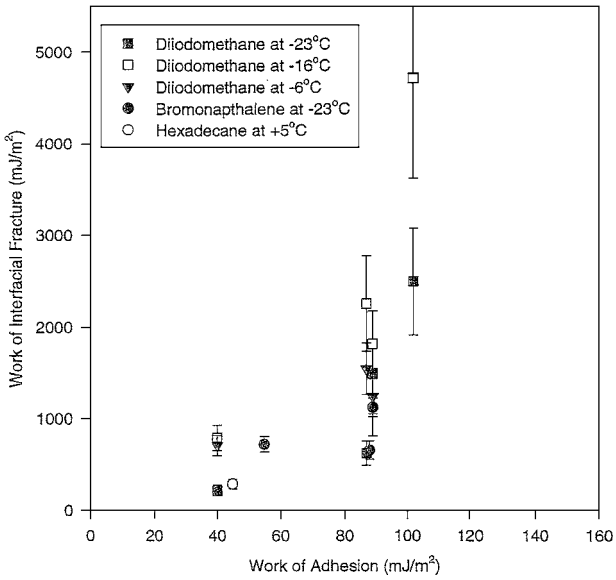

Figure 5 Plot of work of fracture, $\boldsymbol{F}$, versus W_a for hydrophobic adhesives on various substrates. Hydrophobic adhesives adhere only by dispersion interactions. The increase in $\boldsymbol{F}$ appears to be exponential.

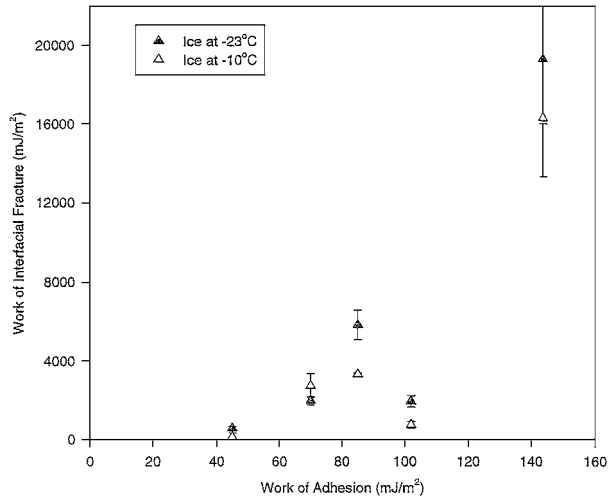

Figure 6 Plot of work of fracture, $\boldsymbol{F}$, versus W_a for hydrophilic adhesive, ice, on various substrates. Ice adheres by hydrogen bonding in addition to dispersion (London) interactions. The increase in $\boldsymbol{F}$ appears to be exponential.

while Fig. 6 shows $\boldsymbol{F}$ versus W_a for the hydrophilic adhesive, ice. (Data obtained at different temperatures are plotted together in these figures, because no significant effect of test temperature was found over the temperature range used.) In both figures, $\boldsymbol{F}$ increases dramatically with W_a, and the appearance of the plots suggested an exponential increase in $\boldsymbol{F}$ with W_a.

Following this suggestion, we plotted the data on semi-logarithmic axes. This is shown in Fig. 7, where data from both hydrophobic and hydrophilic adhesives are plotted together. The symbols have the same meanings as in Figs 5 and 6, with the addition of open diamonds to represent data for ice on various substrates obtained by another experimenter, who used a slightly different pressurization rate [6]. A linear regression through the points in Fig. 7 was performed, and a correlation coefficient, R, of 0.81 was obtained. According to the principles of statistics, the value of R^2 represents

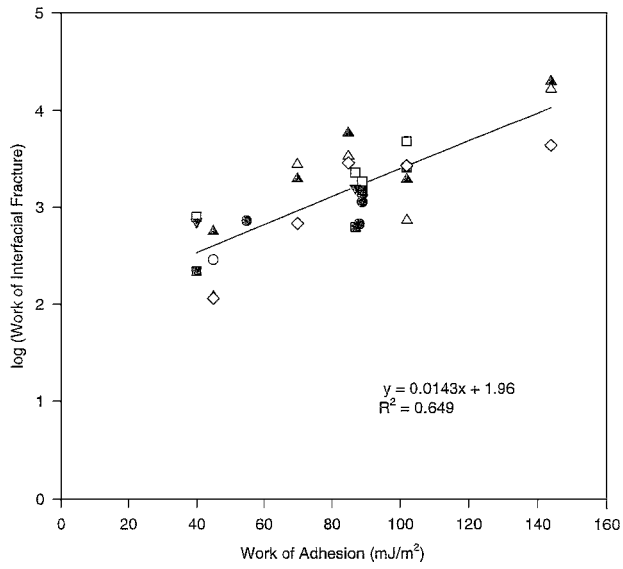

Figure 7 Plot of log(Work of fracture) versus work of adhesion, W_a, for all adhesive-substrate combinations. $\boldsymbol{F}$ is work of fracture. Linear regression gave the straight line shown and a correlation coefficient, R, of 0.81.

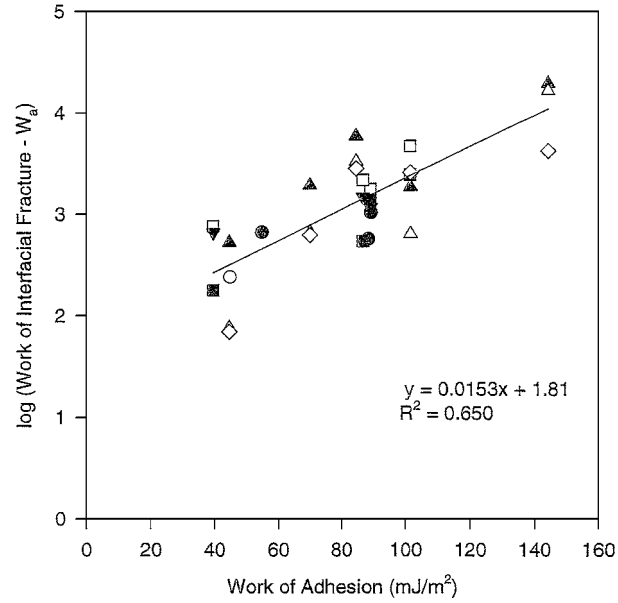

Figure 8 Plot of log(work of fracture $-W_a$) versus work of adhesion, W_a, for all adhesive-substrate combinations. The quantity (work of fracture $- W_a$) is the dissipated energy contained in the work of fracture, $\boldsymbol{F}$. Linear regression gave the straight line shown and a correlation coefficient, R, of 0.81.

the portion of variation in log$\boldsymbol{F}$ that can be explained by W_a. Thus, 65% of the variation in log$\boldsymbol{F}$ can be explained by variation in W_a, while the remaining 35% is due to other factors. From the equation of the straight line in Fig. 7, the relation between $\boldsymbol{F}$ and W_a was determined to be $\boldsymbol{F} = 91.3(e^{0.033W_a})$.

The excess of $\boldsymbol{F}$ over W_a, expressed as $(\boldsymbol{F} - W_a)$, also increases exponentially with W_a, as shown in Fig. 8. A plot of $\log(\boldsymbol{F} - W_a)$ versus W_a gives a straight line with a positive slope and a correlation coefficient of 0.81. Similar to the case of log$\boldsymbol{F}$ versus W_a, 65% of the variation in $\log(\boldsymbol{F} - W_a)$ can be explained by W_a. From the equation of the straight line in Fig. 8, the relation between $(\boldsymbol{F} - W_a)$ and W_a was determined

to be $(\boldsymbol{F} - W_a) = 64.6(e^{0.035W_a})$. The similarity of this equation to the one above is to be expected, because $(\boldsymbol{F} - W_a)$ is contained within $\boldsymbol{F}$ and is nearly equal to it.

Parenthetically, we note that the equations above are not ones that can be extended over a wider range of W_a, starting at zero and extending to infinity. Only a limited range of W_a has any physical meaning, and the values of the adhesive-substrate interfaces used in our study span a major portion of that range. The range of W_a is set by the electron densities and nuclear charges of the atoms in the adhesive and in the substrate. In other words, the range for W_a (at ambient temperatures) is essentially set by the periodic table. The lower limit is about 24 mJ/m^2, exemplified by interfaces between a hydrocarbon and a fluorocarbon or between two fluorocarbons. These materials contain atoms of the lowest possible nuclear charge and electron density and have the lowest possible densities in the condensed state. The upper limit would necessarily be set by metal-metal interfaces, since metals have the highest possible electron densities, nuclear charges, and physical densities. A typical upper-limit value is 480 mJ/m^3, determined from the measured contact angle of liquid mercury on silver [18]. Values of W_a between 144 mJ/m^2 and 480 mJ/m^2, which could be achieved by various combinations of metals and ceramics, have not been explored by means of contact angle measurements, because metals and ceramics other than mercury do not exist in liquid form at ambient temperatures.

It is intuitive that interfaces characterized by higher W_a-values should be able to withstand higher levels of stress before separation and therefore would give higher values of $\boldsymbol{F}$. However, the notable feature that emerges from the plotting schemes presented in Figs 7 and 8 is that $\boldsymbol{F}$ and $(\boldsymbol{F} - W_a)$ increase *exponentially* with W_a. Exponential behavior typifies phenomena that increase in proportion to the amount that has already occurred, and the only examples of such phenomena in mechanical behavior are orientation hardening in polymers and strain hardening in metals. Thus we are led to conclude that orientation or strain hardening is the process underlying the observed increase in $\boldsymbol{F}$ and $(\boldsymbol{F} - W_a)$ with W_a.

In a paper on the theoretical aspects of interfacial fracture [19], Wei and Hutchinson used the cohesive zone model to establish the exponential relation between total work of fracture and W_a in the presence of strain hardening. In the cohesive zone model, the interface is regarded as a fracture process zone with its own characteristic work of fracture, Γ_o, and maximum separation stress, $\hat{\sigma}$, which are uniquely related to each other by a traction-separation law devised for the model. Since, in Ref. 19, Γ_o is used to designate separation energy in the *absence* of irreversible processes of any kind, it is equivalent to W_a used by us in the present work. While we concede that the different adhesive-substrate interfaces used in our study might not have identical traction-separation laws, they are not likely to differ vastly and can be assumed identical for the sake of argument. Wei and Hutchinson showed that, for a given traction-separation law, increasing Γ_o (i.e., W_a) corresponds to increasing $\hat{\sigma}$, and, when strain hardening occurs an increase in $\hat{\sigma}$ brings about an *exponential* increase in the total work of fracture, $\boldsymbol{F}$.

For the interfaces examined in our study, the absence of evidence for permanent deformation in the bulk adhesive or substrate suggested that the orientation (strain) hardening must occur in the interfacial region and must involve a small enough volume of material to escape visual detection at low magnification. The location of the orientation hardening was further pinpointed by the fact that the low-molecular-weight adhesives used in our study were brittle in the solid state and had neither the molecular connectivity of polymer chains nor the ductility of metals. In other words, the *adhesives* used in our study lacked the capability to undergo a process such as orientation hardening. This led to the conclusion that the substrates (polymer or metal), and not the adhesives, were exhibiting the orientation hardening.

An idea of the length scale, or process length, over which a process such as orientation hardening occurs can be had from a material-based length quantity, L, described in Ref. 19. This length is given by

$$L = \frac{E \cdot \Gamma_o}{3\pi(1 - \nu^2)\sigma_Y^2}, \tag{9}$$

where E, ν, and σ_Y, are the elastic modulus, Poisson's ratio, and yield or elastic strength of the material in which the irreversible, energy-consuming process of interest takes place. As mentioned before, because of the way Γ_o is defined in Ref. 19, it can be replaced by W_a. To compute approximate values of L for the polymer substrates in our study, we used representative values of 50 mJ/m^2, 1.5 GPa, and 85 MPa for W_a, E, and σ_Y, respectively. For the steel substrate, we used representative values of 70 mJ/m^2, 33 GPa, and 600 MPa for W_a, E, and σ_Y, respectively. The results for L are 1.2 nm (polymers) and 0.75 nm (steel). These length scales are minimum values for each material and are too small to be detected optically. However, continued orientation hardening would progressively increase E in Equation 9, causing concomitant increases in L. In the absence of fracture, the process of orientation hardening could continue until its length scale extended into the bulk of the specimen. In our study, the weak interfaces led to fracture of the specimens before the length scale of the permanent deformation due to orientation hardening could reach a detectable value (i.e., tenths of a micron by optical microscopy). Therefore, we can conclude that the orientation hardening responsible for the excess energy of fracture in our specimens occurred within a layer no more than tenths of a micron from the interfacial plane.

5. Conclusion

A study of the relation between total work of fracture, $\boldsymbol{F}$, and the thermodynamic work of adhesion, W_a, was conducted on bimaterials systems that exhibited fracture at the interface. The independent variable, W_a, ranged from about 40 mJ/m^2 to 144 mJ/m^2. The dependent

variable, $\boldsymbol{F}$, ranged from 0.12 J/m^2 to 20 J/m^2, with most values falling below 5 J/m^2. Since thermodynamic work of adhesion, W_a, represents the energy required for reversible separation of the two materials at the interface, and since $\boldsymbol{F}$ includes the energy required for both reversible and irreversible processes during separation, the excess of $\boldsymbol{F}$ over W_a represents the energy consumed by the irreversible processes that occur in the specimen during loading and fracture. This excess, $(\boldsymbol{F} - W_a)$, was found to increase exponentially with W_a and was attributed to orientation hardening of the substrate within a very thin layer adjacent to the interfacial plane.

The lesson to be learned from this study is that even for the simplest and weakest interfaces, irreversible processes can occur within the interfacial region during loading and fracture, causing experimentally determined values for work of fracture to exceed the thermodynamic work of adhesion.

Acknowledgements

The authors acknowledge very helpful discussions with Prof. Kenneth Liechti of the University of Texas and with Prof. David Dillard of Virginia Polytechnic Institute and State University.

References

1. M. SCHRADER, *J. Colloid Interface Sci.* **213** (1999) 602.
2. M. L. WILLIAMS, *J. Appl. Polym. Sci.* **14** (1970) 1121.
3. J. D. BURTON, W. B. JONES and M. L. WILLIAMS, *Trans. Soc. Rheology* **15** (1971) 39.
4. M. L. WILLIAMS, *J. Adhesion* **5** (1973) 81.
5. K. R. JIANG and L. S. PENN, *ibid.* **32** (1990) 203.
6. *Idem.*, *ibid.* **32** (1990) 217.
7. M. FERNANDO and A. J. KINLOCH, *Int. J. Adhesion & Adhesives* **10** (1990) 69.
8. H. DANNENBERG, *J. Appl. Polym. Sci.* **14** (1961) 125.
9. B. M. MALYSHEV and R. L. SAGALIK, *Int. J. Fracture Mechanics* **1** (1965) 114.
10. S. J. BENNETT, K. L. DEVRIES and M. L. WILLIAMS, *Int. J. Fracture* **10** (1974) 33.
11. E. H. ANDREWS and A. STEVENSON, *J. Mater. Sci.* **13** (1978) 1680.
12. B. MILLER, L. S. PENN and S. HEDVAT, *Colloids and Surfaces* **6** (1983) 49.
13. L. S. PENN and C. T. CHOU, *J. Compos. Technol. Research* **12** (1990) 164.
14. B. W. CHERRY, "Polymer Surfaces" (Cambridge University Press, Cambridge, 1981) Ch. 2.
15. K. M. LIECHTI and A. SHIRANI, *Int. J. Fracture* **67** (1994) 21.
16. A. SHIRANI and K. M. LIECHTI, *ibid.* **93** (1998) 281.
17. K. M. LIECHTI, A. SHIRANI, R. G. DILLINGHAM, F. W. BOERIO and S. M. WEAVER, *J. Adhesion* **73** (2000) 259.
18. L. S. PENN, unpublished results.
19. Y. WEI and J. W. HUTCHINSON, *Int. J. Fracture* **93** (1998) 315.

Received 11 April
and accepted 18 September 2001